DISPERSIVE CORRECTIONS TO A MODULATION THEORY FOR STRATIFIED GRAVITY WAVES

RAZVAN C. FETECAU * AND DAVID J. MURAKI †

Abstract. Modulation theories, as used to describe the propagation of wavetrains, often possess a natural limitation in their tendency to finite-time breakdown via a wavenumber shock that occurs with the crossing of characteristics. For the geophysical example of linear wave propagation in an inviscid, density-stratified fluid, we demonstrate that the asymptotic corrections to modulation theory are sufficient for short-time regularization of the wavebreaking singularity. Computations show that the shock development is pre-empted by the emergence of spatial oscillations. In the asymptotic limit, these oscillations display a self-similar collapse of scale both in space and in time. Finally, an envelope analysis following a characteristic demonstrates that these new correction terms act locally as second-order wave dispersion.

Key words. inertia gravity waves, modulation theory, regularization of wavebreaking.

AMS subject classifications. 74J40, 76B70, 76M45

1. Introduction. Modulation theory, as presented in Whitham [41], is one of several closely related asymptotic methods that can be applied to dispersive wave systems. The theory describes the time evolution of slowly-varying wavetrains – specifically, waveforms characterized by near-periodicity in both space and time. At the core of the theory are familiar principles of conservation of phase and wave action [3, 5] that are mathematically expressed as systems of hyperbolic conservation laws involving the physical wave parameters (i.e. wavenumber, frequency, amplitude, background inhomogeneities, etc.) [38]. Modulation theory generalizes the amplitude equation method for quasi-monochromatic wavepackets [25] to incorporate order one changes in wavenumber and frequency. However, as a strongly nonlinear theory, it is also the case that many modulation theories possess a natural limitation in their tendency to finite-time breakdown via a wavenumber shock that occurs with the crossing of characteristics [10, 21]. This article explores a particular example where asymptotic corrections that introduce dispersion into the modulation theory can significantly alter the steepening process that precedes the shock singularity.

The canonical example of the crossing of characteristics is the inviscid Burgers equation. It is also a common starting point for understanding the idea of regularization, whereby additional terms can defer, or suppress the development of a singularity. This is the thesis behind the original Burgers equation [15], where weak viscous dissipation saturates the wave steepening by the formation of front-like spatial structures. In non-dissipative systems, regularization can occur with the appearance of spatial oscillations arising from the radiation of dispersive waves [17]. The Korteweg-deVries equation provides a basic illustration for such dispersive regularization [19]. For a modulation theory based upon an underlying PDE dynamics, it is a reasonable expectation that regularization terms might derive from the natural asymptotic corrections. In this paper, we demonstrate a systematic derivation of asymptotic corrections to a modulation theory for a dispersive wave system.

This article is an asymptotic study of the modulation theory applied to the specific

*Mathematics Department, Simon Fraser University, 8888 University Drive, Burnaby BC Canada, V5A 1S6 (van@math.sfu.ca).

†Mathematics Department, Simon Fraser University, 8888 University Drive, Burnaby BC Canada, V5A 1S6 (muraki@math.sfu.ca).

geophysical example of linear wave propagation in an inviscid, density-stratified fluid. Our choice of the Boussinesq system is motivated by the goal of understanding the breakdown of stratospheric waves [9, 27]. As an asymptotic analysis, the choice of modulation theory is particularly appropriate for atmospheric gravity waves, as the vertical variations in profiles of density stratification and horizontal wind shear from surface to stratosphere, while often significant, are typically slowly-varying [7, 11]. The modulation theory for the fully nonlinear Boussinesq equations was established in works by Bretherton [4, 5] and Grimshaw [11]. The important fluid dynamical effect with the inclusion of nonlinearity is the interaction of the waves with the mean flow. However, our early attempts to understand the breakdowns of the fully nonlinear Boussinesq by an extension of modulation theory revealed two challenges: first, to develop a systematic asymptotic derivation of the corrections to modulation theory in the setting of a PDE system; and second, to interpret the large number of correction terms for their impact on the wave propagation.

As an initial step, we embarked upon a restricted analysis that focussed only on the linear corrections. As discussed in Whitham, the derivation of correction terms to modulation theory is trivial for scalar wave PDEs, however the vector-based treatment here is developed for future application to the nonlinear problem. This adaptation to the vector PDE system, while classical in approach, does not seem to exist within the modulation theory literature. Nonlinear corrections have been considered by Tabaei and Akylas [34], but the linear dispersive corrections were limited to quasi-monochromatic effects. In this article we develop, within the linear context, a methodology for fully addressing the case of strong modulations. In particular, we confirm that the full dispersive corrections are sufficient, at least for short times, to regularize the singular wavebreaking — and with a self-similar dynamics that differs from more familiar dispersive paradigms, like the KdV equation. The continuation of this analysis as applied to the nonlinear Boussinesq system is discussed in the closing section.

This analysis of modulation theory begins with the concrete illustration of a modulated wavetrain evolving towards a wavenumber shock. It is then shown numerically that our corrected version of modulation theory gives short-time regularization past the leading-order singularity time. In Section 3, a systematic multiple-scale derivation of modulation theory is developed for producing these next-order correction terms. After verifying computationally that next-order accuracy has indeed been achieved with the correction terms, it is shown, by direct comparison with the PDE solution, that the the shock development is pre-empted by the emergence of short-scale spatial oscillations (Section 4). A series of computations towards the asymptotic limit reveal that this oscillatory spatial structure displays a self-similar collapse of scale both in space and in time. Furthermore, the initial onset of short-scales do not invalidate the long-wave assumption under which modulation theory rests. As a generalization to quasi-monochromatic wavepackets, in Section 5, an envelope analysis following a characteristic verifies that these corrected modulation equations act locally as second-order wave dispersion.

2. Shock Regularization of an Inertia Gravity Wavetrain. A modulated wavetrain is the generalization of a Fourier wave that allows the wavevector and amplitude to be slowly-varying on scales much longer that the wavelength. Such wavetrains naturally occur from wave radiation from a localized source as the generic long-time outcome of group velocity kinematics [37]. Modulations can also be caused by long-scale changes of the background medium [2, 3]. In this Section, we introduce

the linear equations for a two-dimensional, inviscid and Bousssinesq fluid, and then present a concrete application of modulation theory to an inertia gravity wavetrain.

Under the Boussinesq assumption, the density effects are incorporated as a buoyancy acceleration in the vertical momentum equation, while the flow velocity is taken to be non-divergent [23, 35]. In two dimensions (x, z), the linearized fluid equations can be written as

$$\eta_t + \bar{u}\,\eta_x \; + \qquad b_x = 0 \tag{2.1a}$$

$$b_t + \bar{u}\,b_x \; - \; N^2\,\psi_x = 0 \tag{2.1b}$$

$$\psi_{xx} + \psi_{zz} \; - \qquad \eta \; = 0 \tag{2.1c}$$

where $\eta(x, z, t)$ denotes vorticity, and $b(x, z, t)$ is the buoyancy disturbance. Incompressibility is imposed through the streamfunction $\psi(x, z, t)$ relation to the horizontal wind, $u = \psi_z$, and vertical motion, $w = -\psi_x$. The two environmental parameters are: $\bar{u}$, a horizontal mean flow; and N, the Brunt-Väisälä frequency that is associated with a stable (light over heavy) background of density stratification. For a uniformly stratified fluid, we take N to be constant and by rescaling time, we can assume $N = 1$. We also simplify by assuming a uniform mean flow, and by changing to a co-moving frame, we can take $\bar{u} = 0$. We remark that the above treatment of the mean flow is not permissible in the nonlinear case because of mean flow coupling [33, 34]. The resulting constant coefficient problem (2.1) now permits an exact gravity wave dispersion relation

$$\omega^2 = \frac{k^2}{k^2 + m^2} \tag{2.2}$$

for wavevector, $\vec{k} = (k, m)^T$, and frequency, ω. As vertical propagation is our primary concern, we take k to be constant, and consider only modulations of the vertical wavenumber m. Hence, our wavetrains are an exact Fourier mode in the horizontal, so that all fields of (2.1) have the form $b(x, z, t) \to b(z, t)\, e^{ikx}$, etc.

The evolution of (2.1) for a modulated (in z) wave experiencing a wavenumber shock is illustrated by the oscillatory fields in Figures 2.1a-c (thin solid curves). The modulations in the initial wavetrain (Figure 2.1a) are evident from the non-uniform wavelength and the (slight) bulges in the amplitude. However, the precise details of this initial condition are deferred to the end of this section, after we have defined suitable modulation variables. The field shown is buoyancy, $b(z, t)$, at times $t = 0, 120, 130$ that illustrate the initial wave, onset of the shock, and just beyond the modulation theory shock time. The solution has been computed by spectral FFT according to the dispersion relation

$$\omega = -\frac{k}{\sqrt{k^2 + m^2}} \qquad ; \qquad c = \frac{\partial \omega}{\partial m} = -\frac{m\omega^3}{k^2} \tag{2.3}$$

as derived from (2.1), with $\bar{u} = 0$ and $N = 1$. The negative square root branch for (2.3) gives positive group velocity, so that modulated features drift to the right. In this example, the initial wave has sections of longer and shorter waves. The longer waves, which have the faster group velocity, tend towards overrunning the shorter waves. This is accompanied by a localized increase in the wave amplitude (Figure 2.1b,c) – and is the qualitative description of a *wavenumber shock*. As the underlying equation (2.1) is linear, this shock does not correspond to any true singular behavior of the PDE.

Modulation theory assumes wavetrain properties vary on a long spatial scale, $\zeta = \epsilon z$, and evolve on a slow time scale $\tau = \epsilon t$, where ϵ is small [5]. For a linear system, the modulations are sinusoidal [39] and the wavetrain is completely specified by the time evolution of the wavenumber, $m(\zeta, \tau)$, and the real-valued amplitude, $A(\zeta, \tau)$. This evolution is governed by two principles: conservation of waves and conservation of wave action ($\mathcal{F} = A^2/\omega$). Mathematically, these can be expressed as the pair of hyperbolic wave equations

$$m_\tau + \quad \omega_\zeta = 0 \tag{2.4a}$$

$$\mathcal{F}_\tau + (c\,\mathcal{F})_\zeta = 0 \tag{2.4b}$$

where $c(m) = \partial\omega/\partial m$ denotes the linear group velocity [41]. The significance of the group velocity explicitly arises as the characteristic speed for both of the above quasi-linear equations [38]. For a homogeneous fluid ($\omega = \omega(m)$ only, with $\bar{u}$ and N constant), it follows from (2.4a) that the group velocity satisfies the kinematic law

$$c_\tau + c\,c_\zeta = 0 \tag{2.5}$$

which is the inviscid Burgers equation. In this case, we have an exact formula for the wavebreaking time of modulation theory

$$\tau_b = -\,\frac{1}{\min\limits_{\zeta} c_\zeta(\zeta, 0)} \tag{2.6}$$

as determined by the initial conditions. Lastly, note that the wavenumber equation (2.4a) is decoupled from the wave action equation (2.4b).

The example of Figure 2.1 is a periodic wavetrain with 24 oscillations on the periodic domain $-24\pi \le z \le 24\pi$, and $\epsilon = 1/24$ is small. The initial wavenumber has a sinusoidal modulation $m(\zeta, 0) = 1 + (1/3)\sin\zeta$, as defined on the long scale $-\pi \le \zeta \le \pi$. The amplitude of the wave envelope, $A(\zeta, 0)$, is indicated in both upper and lower envelopes in the initial condition (Figure 2.1a), and is chosen to make the wave action initially uniform, $\mathcal{F}(\zeta, 0) = -1$. The initial group velocity, as calculated with (2.3), appears in the lower plot of Figure 2.1a. For this initial condition, the breaking time from (2.6) for modulation theory is $\tau_b \approx 5.24$, which for $\epsilon = 1/24$, corresponds to $t_b \approx 125.75$. Just prior to the wavebreaking time $t = 120 < t_b$, the wave amplitude $A(\zeta, \tau)$ and group velocity $c(\zeta, \tau)$, as evolved from the modulation equations (2.4 with 2.3), are shown as the lower envelope and the group velocity plot (light dashed curves, Figure 2.1b). The near-singular group velocity curve shows the distinctive pre-break steepening, and coincides with a near-cusp singularity in the amplitude. The upper envelope (dark solid curve, Figure 2.1b), however, better follows the oscillations of the wavetrain — this is the amplitude predicted by our dispersion-corrected modulation theory (Section 3). Finally, Figure 2.1c establishes that the corrected theory (dark solid curves) not only can regularize the singularity of modulation theory, but also continues to give very good agreement for the wave envelope past the wavebreak time ($t = 130 > t_b$) . Oscillations that appear as part of the shock regularization are apparent in both the amplitude and group velocity; these are further investigated in Section 4.

3. Derivation of The Modulation Equations. Several general discussions of higher-order extensions for modulation theory appear in the early literature [22, 2, 40], yet do not seem to have found use in applications. Here, we adopt the perspective

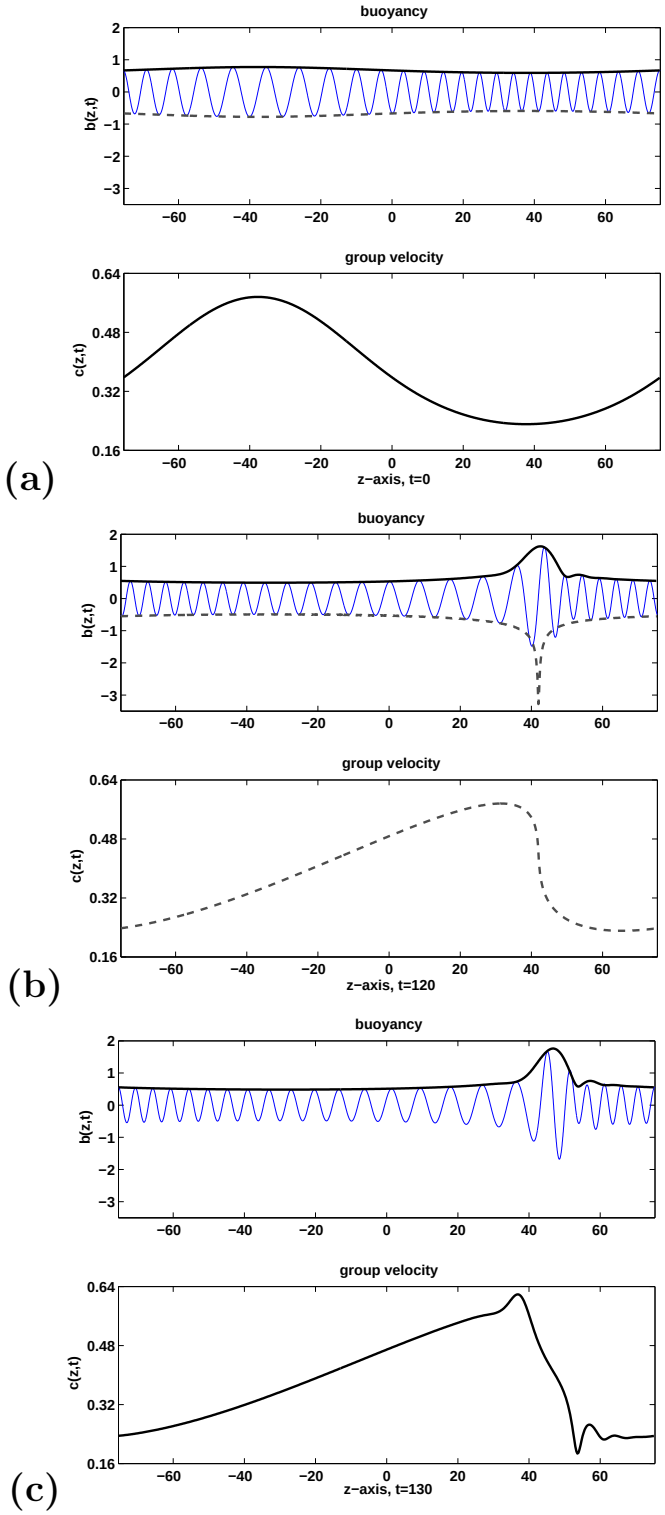

FIG. 2.1. *Three times in the evolution of a wavetrain with a wavenumber shock: (a) $t = 0$ initial condition, (b) $t = 120$ onset of the shock, and (c) $t = 130$ just past the leading-order shock time, $t_b \approx 125.75$ ($\tau_b \approx 5.24$). The top plot of each panel (a-c) shows the oscillatory buoyancy field (thin solid) from (2.1). The amplitude envelopes (top plots, a-c) and group velocity (bottom plots, a-c) are as predicted by modulation theory (light dashed), and the dispersion-corrected theory (dark solid). Note the near-singular steepening of the group velocity with the shock onset, and the appearance of dispersive oscillations afterwards.*

illustrated in Whitham ([41], chap 15.5) whereby the dispersion relation includes next-order corrections from (slow) gradients of the wave parameters. In particular, we devise an approach that includes only spatial gradients, so that the first-order in time nature of the modulation theory is preserved.

We consider a sinusoidal wavetrain solution to (2.1 with $N = 1$ and $\bar{u} = 0$) that contains just a single wavenumber in the x-direction,

$$\begin{pmatrix} b \\ \eta \\ \psi \end{pmatrix} = \mathrm{Re}\left\{ \mathbf{a}(z,t)\, e^{i\phi(z,t)}\; e^{ikx} \right\} \tag{3.1}$$

and with spatial modulations only in the z-direction. Both the phase ϕ and vector amplitude $\mathbf{a}$ are taken to be real-valued. The generalized wavenumber and frequency are defined by the phase gradients

$$m(\zeta,\tau) \equiv \phi_z \qquad ; \qquad \omega(\zeta,\tau) \equiv -\phi_t \tag{3.2}$$

that, with the vector amplitude $\mathbf{a}(\zeta,\tau)$, are assumed to depend on the slow variables $\zeta = \epsilon z$ and $\tau = \epsilon t$. Equality of the mixed partials in terms of the slow scales gives the first of the conservation laws (2.4a).

Substitution of the wavetrain ansatz (3.1) into the linear Boussinesq system (2.1) gives a slow-scale equation for the vector amplitude $\mathbf{a}(\zeta,\tau)$

$$[\mathcal{M} + \epsilon\mathcal{L}_1 + \epsilon^2\mathcal{L}_2]\,\mathbf{a} = \mathbf{0}, \tag{3.3}$$

with the matrix operators

$$\mathcal{M} = \begin{bmatrix} k & -\omega & 0 \\ -\omega & 0 & -k \\ 0 & -k & -k\,(k^2+m^2) \end{bmatrix}, \tag{3.4}$$

$$\mathcal{L}_1 = i \begin{bmatrix} 0 & -\partial_\tau & 0 \\ -\partial_\tau & 0 & 0 \\ 0 & 0 & k\,(2m\partial_\zeta + m_\zeta) \end{bmatrix}, \tag{3.5}$$

$$\mathcal{L}_2 = \begin{bmatrix} 0 & 0 & 0 \\ 0 & 0 & 0 \\ 0 & 0 & k\,\partial_\zeta^2 \end{bmatrix} \tag{3.6}$$

and ∂_τ and ∂_ζ denote derivatives on the slow-scales. Note that the equation for the streamfunction inversion (2.1c) has been multiplied by ik to give a symmetric leading order matrix $\mathcal{M}$. Without modulations, the exact plane wave solutions are the homogeneous solutions to $\mathcal{M}\mathbf{a}_N = \mathbf{0}$, for which the zero determinant condition

$$\omega^2 = \frac{k^2}{k^2+m^2} \equiv \Omega(m)^2 \tag{3.7}$$

recovers the gravity wave dispersion relation (2.3), with the nullvector

$$\mathbf{a}_N = \begin{pmatrix} 1 \\ k/\omega \\ -\omega/k \end{pmatrix}. \tag{3.8}$$

We now use $\Omega(m)$ to denote the linear dispersion relation (3.7), to distinguish from the corrected frequency, ω, which has the former as the leading-order. We likewise identify the group velocity

$$c = c(m,\omega) = \frac{\partial \omega}{\partial m} = -\frac{m\omega^3}{k^2} \tag{3.9}$$

as distinguished from its leading-order

$$C = c(m,\Omega) = -\frac{m\Omega^3}{k^2}. \tag{3.10}$$

Note that the sign for the square root branch of the dispersion relation (3.7) is implicit in the above definitions of group velocity.

To go beyond modulation theory, we anticipate an adjustment of the frequency, ω, through the introduction of an $O(\epsilon^2)$ correction to the leading-order operator $\mathcal{M}$. A regularizing correction R now appears in the modified matrix

$$\begin{aligned} \mathcal{M}_R &= \begin{bmatrix} k & -\omega & 0 \\ -\omega & 0 & -k \\ 0 & -k & -k\,(k^2+m^2+\epsilon^2 R) \end{bmatrix} \\ &= \begin{bmatrix} k & -\omega & 0 \\ -\omega & 0 & -k \\ 0 & -k & -k^3/\omega^2 \end{bmatrix} \end{aligned} \tag{3.11}$$

where the second form derives from the assumption of the new zero-determinant condition

$$\omega^2 = \frac{k^2}{k^2+m^2+\epsilon^2 R}. \tag{3.12}$$

The above choice for the regularizing correction is advantageous as it leaves the nullvector (3.8) unchanged, and exact (up to the known asymptotic accuracy of ω via R). The slow-scale equation (3.3) becomes

$$\left[\mathcal{M}_R + \epsilon\mathcal{L}_1 + \epsilon^2\mathcal{L}_{2R}\right]\mathbf{a} = 0, \tag{3.13}$$

where the regularization term is added back into the $O(\epsilon^2)$ operator

$$\mathcal{L}_{2R} = \begin{bmatrix} 0 & 0 & 0 \\ 0 & 0 & 0 \\ 0 & 0 & k\,(\partial_\zeta^2 + R) \end{bmatrix}. \tag{3.14}$$

Upon introducing a perturbation expansion of the vector amplitude $\mathbf{a}$, the regularizing term, R, will be determined by a solvability condition at $O(\epsilon^2)$. Overall, the following presentation of modulation theory is structured in the fashion of a linear WKB calculation [2, 24]. The singular (matrix) condition yielding ω serves as the eikonal relation, and the solvability condition for $\mathbf{a}$ provides the transport equation [1]. The regularization strategy is similar in spirit to the method of Poincaré-Lindstedt, whereby the frequency imbedded in the leading-order operator is expanded to have deferred corrections [18].

The first term in the perturbation expansion for the vector amplitude

$$\mathbf{a} = A(\zeta,\tau)\;\mathbf{a}_N + \epsilon\,\mathbf{a}_1 + \epsilon^2\,\mathbf{a}_2 + \ldots, \tag{3.15}$$

has the direction of the nullvector (3.8), but is arbitrary up to a slowly-varying, real-valued amplitude $A(\zeta,\tau)$. Note that the nullvector (3.8) also contains slow-variations and ϵ-dependence through $\omega(\zeta,\tau)$ (3.12). The $O(\epsilon)$ terms in the slow-scale equation (3.13) give

$$\mathcal{M}_R\,\mathbf{a}_1 + \mathcal{L}_1(A\,\mathbf{a}_N) = 0 \tag{3.16}$$

which the correction $\mathbf{a}_1$ must satisfy. As $\mathcal{M}_R$ is a (symmetric) singular matrix, existence of $\mathbf{a}_1$ requires the solvability condition

$$(\mathbf{a}_N)^{\mathrm{T}}\mathcal{L}_1(\mathcal{A}\,\mathbf{a}_N) = 0 \tag{3.17}$$

and results in the scalar transport equation for the amplitude $A(\zeta,\tau)$

$$\partial_\tau\left(\frac{k}{\omega}A\right) + \frac{k}{\omega}\,\partial_\tau A - \omega\left\{2m\partial_\zeta + m_\zeta\right\}\left(\frac{\omega}{k}A\right) = 0. \tag{3.18}$$

By inspection, A is seen to be an integrating factor for this expression (since k is a constant), allowing a conservation law form

$$\left(\frac{A^2}{\omega}\right)_\tau - \left(\frac{m\omega^3}{k^2}\,\frac{A^2}{\omega}\right)_\zeta = 0. \tag{3.19}$$

Upon the identification of the group velocity (3.9), this recovers the second equation (2.4b) for the wave action $\mathcal{F} = A^2/\omega$,

Continuing to next order in the perturbation requires an explicit representation of $\mathbf{a}_1$. A closed form expression for a particular solution is

$$\mathbf{a}_{1p} = -i\begin{pmatrix} 0 \\ \dfrac{1}{\omega}\left(\dfrac{k}{\omega}A\right)_\tau \\ \dfrac{1}{k}A_\tau \end{pmatrix} \tag{3.20}$$

for which a derivation is included in the Appendix. However, it proves useful to adjust with a specific choice of homogeneous contribution

$$\mathbf{a}_1 \;=\; \mathbf{a}_{1p} + \frac{i}{2}\left(\frac{A}{\omega}\right)_\tau \mathbf{a}_N \;=\; -i\begin{pmatrix} -\dfrac{1}{2}\left(\dfrac{A}{\omega}\right)_\tau \\ \dfrac{k}{2\omega}\left(\dfrac{A}{\omega}\right)_\tau \\ \dfrac{1}{k}A_\tau + \dfrac{\omega}{2k}\left(\dfrac{A}{\omega}\right)_\tau \end{pmatrix} \tag{3.21}$$

that anticipates simplification in the calculation of the regularizing term R. The $O(\epsilon^2)$ terms in the slow-scale equation (3.13) are

$$\mathcal{M}_R\,\mathbf{a}_2 + \mathcal{L}_1(\mathbf{a}_1) + \mathcal{L}_{2R}(A\,\mathbf{a}_N) = 0\ , \tag{3.22}$$

from which the solvability condition for the existence of $\mathbf{a}_2$

$$(\mathbf{a}_N)^{\mathrm{T}}\left\{\mathcal{L}_1(\mathbf{a}_1) + \mathcal{L}_{2R}(A\,\mathbf{a}_N)\right\} = 0 \tag{3.23}$$

determines R. Highlights in this calculation are deferred to the Appendix. Particularly noteworthy is that the choice of homogenous contribution in (3.21) causes all $A_{\tau\tau}$ terms to identically cancel. Our final expression for the regularizing term

$$\begin{aligned} R(m,\omega,A) &\sim \frac{3}{4k^2}\frac{1}{\omega A}(2m\partial_\zeta + m_\zeta)\left\{\omega^2(2m\partial_\zeta + m_\zeta)(\omega A)\right\} \\ &+ \frac{m}{2k^2}(m\omega\omega_\zeta)_\zeta + \frac{1}{4k^2}\left(m\omega_\zeta\right)^2 - \frac{(\omega A)_{\zeta\zeta}}{\omega A} \end{aligned} \tag{3.24}$$

is a form that contains only spatial ζ-gradients.

In summary, our statement of an equation set for a corrected modulation theory remains that of conservation of phase (2.4a) and wave action (2.4b)

$$m_\tau + \omega_\zeta = 0 \qquad ; \qquad \mathcal{F}_\tau + (c\,\mathcal{F})_\zeta = 0 \tag{3.25}$$

but the flux terms are now modified by our extended notion of the frequency dependence (3.12). Because of the multiple-scale nature of the representation (3.1), only the next-order corrections to the phase (via wavenumber m) are necessary to achieve an additional order of accuracy in the physical fields (b,η,ψ). Hence, the only change necessary is the regularization term in the frequency ω via the dispersion relation (3.12)

$$A^2 = \Omega(m)\,\mathcal{F} \tag{3.26}$$

$$\omega^2 = \frac{k^2}{k^2 + m^2 + \epsilon^2 R(m,\Omega(m),A)} \tag{3.27}$$

$$c \;= C(m) = -\frac{m\Omega^3}{k^2} \tag{3.28}$$

where the same square root branch is taken for both ω and Ω. With the addition of the correction term to the dispersion relation, the wavenumber equation is now weakly coupled to the wave action, $\mathcal{F}$.

4. Numerical Results: Asymptotic Accuracy and a Collapse of Scale. We investigate numerically the corrected version of the modulation system (3.25) which is completed with the additional relations (3.26-3.28), and the linear frequency Ω (3.7). The numerical method used is standard, with the spatial derivatives computed pseudo-spectrally and the time-stepping done using 4th-order Runge-Kutta. To study the impact of the correction terms, with the following computations, we

1. validate the next-order asymptotic accuracy,
2. illustrate the scale collapse of the regularization in the weak dispersion limit,
3. quantify a self-similarity in the structure of the dispersive oscillations.

In our numerical experiments we consider the following initial condition for (3.25):

$$m(\zeta,0) = m_0 + \Delta m\,\sin\zeta \tag{4.1a}$$

$$F(\zeta,0) = -1, \tag{4.1b}$$

where m_0 and Δm are constants and $-\pi \le \zeta \le +\pi$. In particular, we have chosen two sets of values for the constants k, m_0 and Δm:

$run1:\quad k = 1/2,\ m_0 = 1,\ \Delta m = 1/3,$

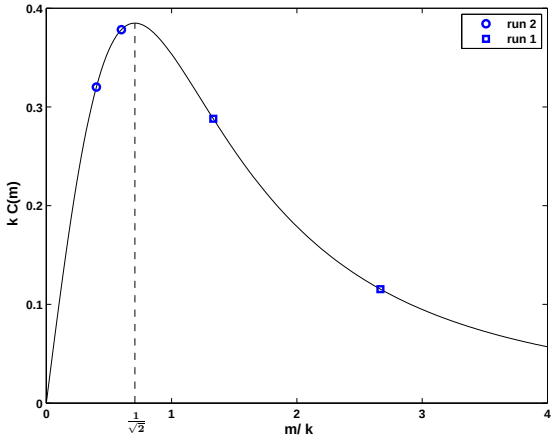

FIG. 4.1. *Plot of normalized group velocity* (kC) *as a function of wavenumber* (m/k) *as obtained from (2.3).*

$$run2: \quad k = 2,\ m_0 = 1,\ \Delta m = 1/5.$$

These two runs are distinguished by having wavenumbers that span two distinct regimes of the group velocity curve. The dispersion relation for stratified waves has a group velocity maximum as a function of vertical wavenumber. A plot of normalized group velocity $kC(m)$ versus wavenumber m/k as given by (2.3) is shown in Figure 4.1. The squares on the group velocity curve correspond to the lowest and highest values of m/k for the initial condition $run1$. In this case, the longer waves are faster, and will overtake the shorter waves – this is the example shown in Figure 2.1. The circles on the curve of Figure 4.1 correspond to the reverse situation where $run2$ has a wavebreaking that occurs with the shorter waves doing the overtaking.

4.1. Asymptotic Accuracy. We confirm the accuracy of the asymptotics by comparing solutions computed from the modulation theories against those of the original Boussinesq system (2.1) with decreasing values of ϵ (1/24, 1/48, 1/96, 1/192). The leading-order and the regularized modulation equations are expected to yield errors in the primitive variables of order $O(\epsilon)$ and $O(\epsilon^2)$, respectively.

The errors between the exact system and the modulation equations are computed in the following way. From the modulation system data, $m(\zeta,\tau)$ and $\mathcal{F}(\zeta,\tau)$, we extract the amplitude $\mathcal{A} = \sqrt{\Omega\mathcal{F}}$ and the phase $\phi(z,t) = \int m\,dz + \phi_0$. Using this amplitude and phase we then reconstruct the primitive variables η and b using (3.1) and the expansion (3.15). The constant of integration, ϕ_0, is obtained by a fit of the reconstructed variables η and b against the corresponding variables from the full Boussinesq system. Both the L^1- and the L^2-norms of the errors in η and b were checked for asymptotic scaling in ϵ.

First, we compute the error norms in η at a time ($\tau = 2.5$), about halfway to the wavebreaking time, well before large gradients appear. The L^2-errors in η from the leading-order (circles) and regularized (triangles) modulation system with the initial condition $run1$ are shown in Figure 4.2. The log-log slopes are consistent with $O(\epsilon)$ and $O(\epsilon^2)$ asymptotic errors. Similar scaling agreement was verified for the L^1-error, and using the buoyancy field, b. Lastly, the squares in Figure 4.2 show the L^2-errors just prior to the wavebreaking time ($\tau = 5$) when the multiple-scale assumptions are

being undermined with the emergence of short scales. Despite that the asymptotic error rate has deteriorated, it still shows errors converging to zero as approximately $\mathrm{O}(\epsilon^{0.75})$. This gives quantitative evidence that the corrected modulation theory is maintaining some predictive ability up to the onset of the wavebreaking event.

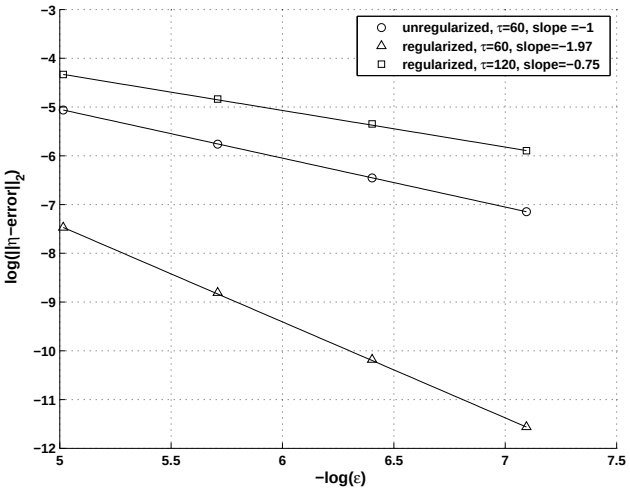

FIG. 4.2. *Log-log plot of the L^2-errors in η for the leading-order and first-order correction modulation equations with initial data corresponding to run1. The leading-order system forms a shock at $\tau_b \approx 5.24$. Computed solutions at $\tau = 2.5$ confirm the leading-order, $O(\epsilon)$, and corrected, $O(\epsilon^2)$, error scalings. At $\tau = 5$ (shortly before τ_b), the regularized system exhibits a weaker convergence of approximately $O(\epsilon^{0.75})$.*

4.2. Collapse of Scale. Our computations of the corrected modulation theory demonstrate the appearance of oscillations preceding the leading-order wavebreaking time. These oscillations, typical of those seen in dispersive systems [17], are shown here to display a self-similar collapse to small-scale spatial structure in the $\epsilon \to 0$ limit. Figure 4.3a shows a sequence of close-ups of the wave action, $\mathcal{F}(\zeta, \tau)$, in the vicinity of the wavebreaking from the initial condition $run1$, but where the ϵ is halved beginning from $\epsilon = 1/24$. For each value of ϵ, these profiles correspond to times $\tau_1(\epsilon) < \tau_b$, defined as the time of first appearance of an oscillation in $\mathcal{F}$ (double zero of $\mathcal{F}_\zeta$, as evident in Figure 4.3b). Having so *synchronized* the spatial profiles, the self-similar nature is revealed by the near-superposition that can be achieved (Figure 4.4a) by a rescaling of the graphs of $\mathcal{F}_\zeta$ (Figure 4.3b). The identical horizontal transformations applied to m_ζ reinforces the self-similarity of the oscillatory structure (Figure 4.4b). This self-similarity is more evident in the derivative field plots, where the effects of long-scale features are lessened. In fact, the superimposition of the m curves is less satisfying — consistent with the observation that the long scale is more strongly apparent on m than F. Nonetheless, there is very good alignment in the locations of the bumps in both curves.

The log-plots of Figure 4.5 reveal clear scaling relationships in this small-ϵ limit. The best fit lines give $\epsilon \to 0$ scalings for the amplitude growth seen in the curves of Figure 4.3

$$|\min \mathcal{F}| \approx \mathrm{O}(\epsilon^{-0.51}) \quad ; \quad |\min \mathcal{F}_\zeta| \approx \mathrm{O}(\epsilon^{-1.3}) \quad ; \quad |\max m_\zeta| \approx \mathrm{O}(\epsilon^{-0.46}) \, . \quad (4.2)$$

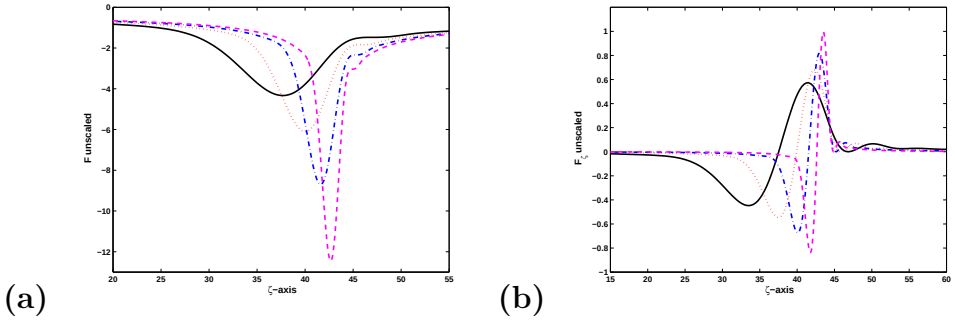

FIG. 4.3. *Vicinity of the emerging oscillations in run*1*, showing (a)* $\mathcal{F}$ *and (b)* $\mathcal{F}_\zeta$ *at the synchronization times* $\tau_1(\epsilon)$*, where all curves of* $\mathcal{F}_\zeta$ *have a double zero. The plots correspond to:* $\epsilon = 1/24$ *(solid),* $\epsilon = 1/48$ *(dotted),* $\epsilon = 1/96$ *(dash-dotted),* $\epsilon = 1/192$ *(dashed).*

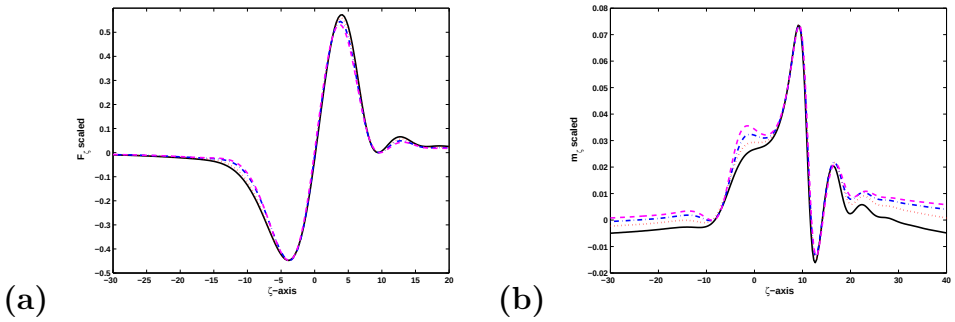

FIG. 4.4. *Rescaled graphs of (a)* F_ζ *and (b)* m_ζ *from Figure 4.3. The scaling landmarks in* $\mathcal{F}_\zeta$ *are* ζ_0 *(circle) and* ζ_m *(square), while for* m_ζ *is the location of the maximum of* m_ζ *(diamond). The reference axes are set by* $\epsilon = 1/24$*. The dispersive waves appear on the leading edge (right) of the wavebreaking zone.*

In addition, both time and space scales (circles and squares of Figure 4.5b) display the self-similar scalings

$$\Delta\zeta(\epsilon) \approx \mathrm{O}(\epsilon^{0.7}) \quad ; \quad \tau_b - \tau_1(\epsilon) \approx \mathrm{O}(\epsilon^{0.66}) \; . \tag{4.3}$$

The space scaling, defined by $\Delta\zeta = \zeta_0(\epsilon) - \zeta_m(\epsilon)$, is based on two landmarks: ζ_0, the zero of $\mathcal{F}_\zeta$ corresponding to the minimum of $\mathcal{F}$; and ζ_m, the location of the minimum of $\mathcal{F}_\zeta$. The time scaling is based upon the synchronization times $\tau_1(\epsilon) \approx \{4.48, 4.75, 4.93, 5.04\}$; so as ϵ decreases, the emergence of waves is occurring on a contracting timescale preceding the breaktime $\tau_b \approx 5.24$.

In the absence of a theory for this self-similar collapse of scale, we performed computations with the KdV equation indicating that power law scalings are also a feature of its weak dispersion limit. In our KdV tests (not shown), it was noted that the scaling exponents were not universal, but indicated steeper collapse rates for later synchronization times. However we know of no theory for this particular collapse in KdV. But to convince ourselves that a similar collapse was occurring in the corrected modulation system, a second set of scalings were calculated for an earlier time $\tau_0(\epsilon) < \tau_1(\epsilon)$, when the first oscillation of m appears. These results, also included in the log-plots of Figure 4.5b (triangles), give the time and space scales

$$\Delta\zeta(\epsilon) \approx \mathrm{O}(\epsilon^{0.66}) \quad ; \quad \tau_b - \tau_0(\epsilon) \approx \mathrm{O}(\epsilon^{0.62}), \tag{4.4}$$

where the time scaling is based upon the synchronization times $\tau_0(\epsilon) \approx \{4.16, 4.54, 4.78, 4.94\}$. As expected, both scalings (4.4) at $\tau_0(\epsilon)$ are seen to be less steep than (4.3) at the later times $\tau_1(\epsilon)$.

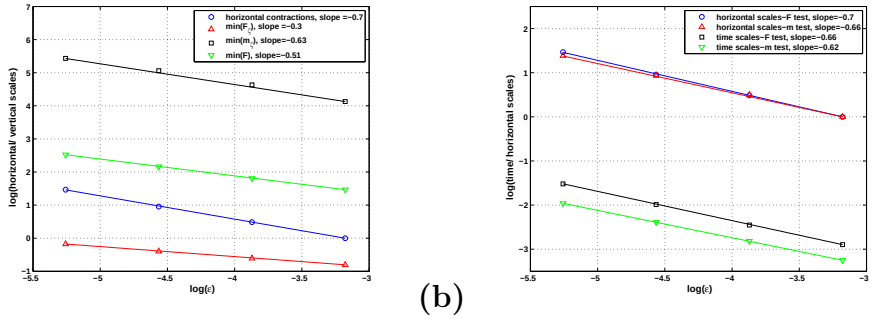

(a) (b)

FIG. 4.5. *Log-plots of amplitudes, space and time scales for run1: (a) amplitude scales (4.2) synchronized to time $\tau_1(\epsilon)$, (b) space and time scales (4.3, 4.4) at times $\tau_0(\epsilon)$ and $\tau_1(\epsilon)$.*

The results obtained for *run2* are similar and we present them briefly. Figure 4.6 shows the rescaled graphs of F_ζ and m_ζ synchronized at $\tau_1(\epsilon)$, and for the same sequence of ϵ. The degree of superposition matches that seen in Figure 4.4 for the computation of *run1*. Common to both *run*1 and *run*2, the wavebreaking involves fast waves overtaking slow waves from left to right, yet these cases differ in that the dispersive oscillations appear ahead of the breaking event in *run*1, and trail in *run*2.

Finally, it is noted that the corrected modulation computations are inherently limited by a linear instability at the high wavenumber end of the spectrum. We have established that this instability only affects scales of $O(\epsilon)$, which is beyond that assumed in the slowly-varying derivation. The computations shown here are spectrally limited below the critical wavenumber. As preliminary computations with nonlinearity indicate the disappearance of this instability, we are optimistic that this annoyance might prove to be an irrelevant detail.

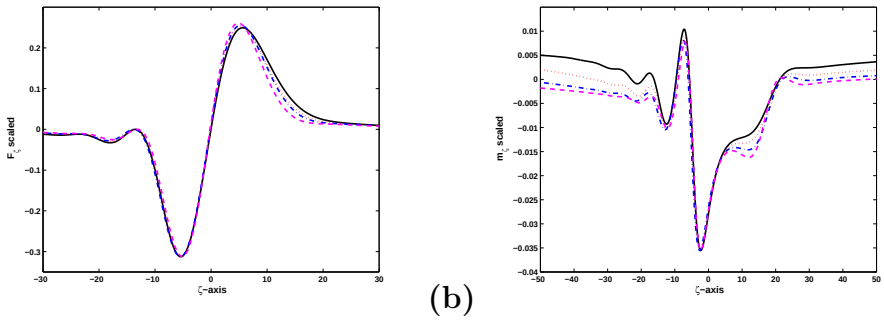

(a) (b)

FIG. 4.6. *Rescaled graphs of (a) F_ζ and (b) m_ζ at the synchronization time $\tau_1(\epsilon)$ for run*2*. Curve labels are as in Figure 4.4. The scaling landmarks for F_ζ (circle and square) are defined as in run*1*, and for m_ζ is the location of the minimum (diamond). Note that the dispersive waves now appear on the trailing edge (left) of the wavebreaking zone.*

5. Dispersion Along a Characteristic. It is a standard result from multiple-scale analysis that the complex envelope of a quasi-monochromatic wavepacket evolves

according to a Schrödinger PDE having the form

$$\Psi_t + \omega' \Psi_z - i\,\epsilon\,\frac{\omega''}{2}\,\Psi_{zz} + \cdots = 0\ . \tag{5.1}$$

The constant coefficients are wavenumber derivatives of the linear dispersion relation $\omega(m)$ evaluated at the carrier wavenumber; specifically, the second-order dispersion of the wavepacket is set by ω'' [25]. In this section, we demonstrate that a similar principle is true of the modulation theory for a Boussinesq internal gravity wavetrain, when following a characteristic.

Following [34], the derivation begins by combining the modulation variables (as defined in Section 3) into a complex-valued amplitude, $\Psi = A\,e^{i\phi}$. It is emphasized that unlike (3.1), Ψ is a scalar quantity. The partial derivatives of $\Psi(z,t)$ are

$$\begin{array}{rcrcl} \Psi_t &=& -i\,\omega(\zeta,\tau)\,\Psi &+& \epsilon A_\tau(\zeta,\tau)\,e^{i\phi} \\ \Psi_z &=& i\,m(\zeta,\tau)\,\Psi &+& \epsilon A_\zeta(\zeta,\tau)\,e^{i\phi} \end{array} \tag{5.2}$$

and involve only slowly-varying quantities. Multiplying the wave action law (3.19) by the complex phase $e^{i\phi}$ gives the rearrangement

$$\epsilon\,\{A_\tau + c\,A_\zeta\}\,e^{i\phi} + \frac{\omega}{2}\left\{\left(\frac{1}{\omega}\right)_\tau + \left(\frac{c}{\omega}\right)_\zeta\right\}\Psi = 0\ . \tag{5.3}$$

The partial derivative expressions (5.2) are used to eliminate the A-derivatives in favor of slow Ψ-derivatives. A dispersion relation identity (6.3) simplifies the last term. Regrouping then gives a reformulation of modulation theory (2.4a, 3.12, 3.19) in the form of an envelope equation

$$\Psi_\tau + \left\{\frac{c}{2}\,\Psi_\zeta + \left(\frac{c}{2}\,\Psi\right)_\zeta\right\} + \frac{i}{\epsilon}\,(\omega - c\,m)\,\Psi = O(\epsilon^2) \tag{5.4}$$

where strong nonlinearity is implied by

$$m(\zeta,\tau) = \mathrm{Im}\left(\frac{\epsilon\,\Psi_\zeta}{\Psi}\right) \tag{5.5}$$

through the m-dependence of ω and c.

With the aim of removing the fast phase, we consider an envelope representation following a leading-order characteristic. As determined by the inviscid Burgers equation (2.5), the characteristics are straight lines along which both c and m are constant (2.4a). Consider then, the representation

$$\Psi = \tilde{\Psi}(\zeta - C_0\tau,\tau)\,e^{(i/\epsilon)(m_0\zeta - \Omega_0\tau)} \tag{5.6}$$

for a moving envelope $\tilde{\Psi}(\zeta - C_0\tau,\tau)$ riding on a carrier wave having the wavenumber m_0 with $\Omega_0 = \Omega(m_0)$. This produces a local-envelope equation

$$\tilde{\Psi}_\tau + \left\{\frac{c - C_0}{2}\,\tilde{\Psi}_{\tilde{\zeta}} + \left(\frac{c - C_0}{2}\,\tilde{\Psi}\right)_{\tilde{\zeta}}\right\} + i\,\left(\frac{\omega - \Omega_0}{\epsilon} - \frac{c\,(m - m_0)}{\epsilon}\right)\tilde{\Psi} = O(\epsilon^2) \tag{5.7}$$

where the spatial variable $\tilde{\zeta} = \zeta - C_0\tau$ follows the group velocity characteristic for the wavenumber m_0. Thus, within an $O(\epsilon)$ vicinity of this central characteristic line, $\tilde{\zeta} = 0$, the fast phase is nullified ($\omega \sim \Omega_0, m \sim m_0$).

To understand the impact of adding the $O(\epsilon^2)$ regularization term, note that the largest contribution occurs within the ω/ϵ factor of (5.7), and contributes at $O(\epsilon)$. The effect can be approximated by the linearization of the corrected dispersion relation (3.12)

$$\omega \sim \Omega - \frac{\epsilon^2}{2}\frac{\omega^3}{k^2}R \tag{5.8}$$

where it remains to re-express the correction R (3.24) in a form that emphasizes its dependence on the gradients of Ψ. A sketch of this final calculation is included in the Appendix, and results in the $O(\epsilon)$-corrected local-envelope equation

$$\tilde{\Psi}_\tau + \left\{ \frac{\Delta c}{2}\,\tilde{\Psi}_{\tilde{\zeta}} + \left(\frac{\Delta c}{2}\,\tilde{\Psi}\right)_{\tilde{\zeta}} \right\} + \left\{ i\left(\frac{\Delta\omega}{\epsilon} - \epsilon\,\gamma\right) - \frac{1}{2}C'(m-m_0)\Omega\left(\frac{1}{\Omega}\right)_{\tilde{\zeta}} \right\}\tilde{\Psi} \\ - \; i\,\epsilon\,\frac{\Omega}{2}\left(\frac{C'}{\Omega}\,\tilde{\Psi}_{\tilde{\zeta}}\right)_{\tilde{\zeta}} = O(\epsilon^2) \tag{5.9}$$

where the phase and group velocity coefficients (relative to the central characteristic values) are

$$\Delta c = (C - C_0) - C'(m - m_0) + O(\epsilon^2) \tag{5.10a}$$

$$\Delta\omega = (\Omega - \Omega_0) - C(m - m_0) + \frac{C'(m-m_0)^2}{2} + O(\epsilon^3)\ . \tag{5.10b}$$

The asymptotic errors in (5.10) apply in the vicinity of the central characteristic ($m - m_0 = O(\epsilon)$, etc.). The only significant addition is the last term of (5.9), which is clearly an analog of the second-order dispersion term in (5.1). Moreover, in a quasi-monochromatic sense, this term will reduce exactly to the Schrödinger form (5.1), as the dispersion-related coefficients assume the values from the central characteristic (m_0, Ω_0, C_0).

Specifically, if we now globally apply the quasi-monochromatic assumption

$$\phi = m_0 z + \tilde{\phi}(\zeta, \tau),$$

the modulated wavenumber is then

$$m = m_0 + \epsilon\tilde{\phi}_\zeta(\zeta,\tau) = m_0 + \epsilon\tilde{m}(\zeta,\tau)\ .$$

Due to this further restriction to small variations, whenever a derivative acts on a modulated variable, it returns an $O(\epsilon)$ quantity. This makes all terms in (5.9) of $O(\epsilon^2)$ or higher, except for a contribution involving $\tilde{\Psi}_{\tilde{\zeta}\tilde{\zeta}\tilde{\zeta}}$. The amplitude equation then reduces to the form (5.1). This re-affirms the quasi-monochromatic analysis for gravity waves of Sutherland [33] and Tabaei and Akylas [34]. It is noteworthy that the sign of the dispersion term in (5.9) is controlled by C' – this is precisely the distinguishing ingredient in the leading versus trailing oscillations seen in *run*1 and *run*2 (Figures 4.4, 4.6).

Of the remaining corrections, those appearing in (5.10) compensate for the divergence of the neighboring characteristics with $\tilde{\zeta} \neq 0$, and γ is the extra phase term from (6.5). Thus, from this analysis, despite the seeming confusion of terms that arise in the regularization (3.24), we confirm that the only new wave dynamics included is that of second-order dispersion. Finally, we note that the derivative forms of the correction terms preserve the structure of the envelope equation (5.9) so that both mass and momentum are locally conserved [25].

6. Closing Remarks. The first motivation for this work was to develop a systematic perturbation approach for developing modulation theory for the PDE system for a stratified gravity wave. While presented for this specific example, the underlying principles are transferable to many other contexts involving modulated waves [26]. The linear example considered here could have been written as a scalar PDE, but we retained the vector nature of the methodology, since such a reduction is typically unavailable for nonlinear systems.

There are two common perspectives for deriving a modulation theory: one is based on variational principles, and the other on multiple-scale analysis. These are understood to be equivalent to leading-order [40]; however, we chose the multiple-scale expansion approach for its ease in representing higher-order corrections of the physical fields (3.15) in terms of the leading-order modulation quantities. As a further guiding principle, our perturbation strategy preserves the underlying physical concepts of conservation of waves and wave action; and hence, subsequent corrections explicitly respect the first-order in time nature of modulation theory. An important technical detail is our use of the homogeneous contribution (3.21) to effect a natural elimination of higher-order time (τ) derivatives, as our choice of normal form [14].

Having obtained an explicit representation of the next-order correction, our second goal was to understand the associated wave physics. Despite the seeming complexity of the correction term, the effects could be attributed to familiar dynamics from the linear dispersion relation. In the case, of nonlinear gravity waves, we expect an unwieldy number of correction terms, and we believed that an understanding of linear propagation alone was an exercise worthy of study.

The present work also provides some insight into an under-addressed issue that is the breakdown of modulated wavetrains. Wave propagation is generically a reversible process, but breakdowns associated with turbulence and mixing is a known mechanism by which gravity waves can irreversibly transport momentum and energy [30]. Therefore, it is equally of interest to understand the failure modes of modulated wave dynamics. To this end, Grimshaw has analyzed the phenomenon of critical level absorption that occurs with the inclusion of weak viscous dissipation [12, 13]. For quasi-monochromatic wavetrains, Sutherland has carried out regime studies that untangle a variety of the known instability mechanisms; two types worthy of note being overturning [31] and convective instability [32].

As a byproduct of this analysis, we have demonstrated numerically that the corrections are sufficient to give short-time regularization of the wavebreaking singularity of modulation theory, and capture well the onset of the dispersive oscillations. The modulation theory here is founded upon the assumption that the wavetrain is described locally as a simple sinusoid in space – however, as is well-known from integrable examples, the crossing of the characteristics is associated with the onset of more complex spatial structure [6, 19, 20]. It is therefore a bit surprising that our corrections, while showing the expected degradation of asymptotic accuracy (Figure 4.2), capture reasonable well the qualitative behavior to time just past the wavebreaking time. One explanation might lie in the fact that the observed exponents of the scale collapse in space are less than one, and hence the wavescale of the dispersive oscillations is still asymptotically longer than the short-scale wavelength – thereby weakly maintaining the slowly-varying assumption.

Looking ahead to the nonlinear Boussinesq equations, the most significant effect is the interaction of the waves with the meanflow. The modulation theory for this fully nonlinear case was established in works by Bretherton [4, 5] and Grimshaw [11].

The extension of these theories to next-order perturbations demand the vector analysis developed here, and a strategy for eliminating higher-order time derivatives that would violate the first-order in time nature of the leading-order modulation theory. In addition, the regularizing corrections would also seem to involve an interaction through second-harmonic waves.

The breakdown of stratified gravity waves featured strongly in a 1978 tank experiment by Plumb and McEwan [29], that was designed as a dynamical analog for an important stratospheric process known as the quasi-biennial oscillation (QBO) [16, 28, 8]. Recently, Wedi and Smolarkewicz [36] have simulated this experiment numerically, and among their findings, have revealed fine details of the phase of the oscillation in which there occurs a turbulent breakdown of an inertia gravity wavetrain. Their computational observations suggest that viscous dissipation and critical level absorption are mechanisms secondary to instabilities from nonlinear flow interactions. It is this line of research that motivates our specific efforts to refine modulation theory applied to atmospheric gravity waves — this paper representing the first inclusion of dispersive corrections.

Appendix.

Derivation of the particular solution (3.20). The nullvector relation $\mathcal{M}_R\,\mathbf{a}_N = 0$ is an identity and can be differentiated with respect to ω. The resulting product rule is also an identity over (ζ,τ), and likewise

$$\frac{i}{2}\left\{A_\tau + \frac{\partial}{\partial\tau}\,A\right\}\left(\mathcal{M}_R\,\frac{\partial\mathbf{a}_N}{\partial\omega} + \frac{\partial\mathcal{M}_R}{\partial\omega}\,\mathbf{a}_N\right) = 0\ .$$

Expanding the operations and simplifying gives

$$i\,\mathcal{M}_R\left(\frac{1}{2}\,A_\tau\frac{\partial\mathbf{a}_N}{\partial\omega} + \frac{1}{2}\left(A\,\frac{\partial\mathbf{a}_N}{\partial\omega}\right)_\tau\right) + \frac{i}{2}\left(\frac{\partial\mathcal{M}_R}{\partial\omega}\,(A\,\mathbf{a}_N)_\tau + \left(\frac{\partial\mathcal{M}_R}{\partial\omega}\,A\,\mathbf{a}_N\right)_\tau\right) = 0$$

where $\partial/\partial\tau = \omega_\tau\,\partial/\partial\omega$ offers some rearrangements. Finally, using the transport equation (3.18), the last two terms are equivalent to $\mathcal{L}_1(A\,\mathbf{a}_N)$, so that by construction

$$\mathbf{a}_{1p} = i\left(\frac{1}{2}\,A_\tau\frac{\partial\mathbf{a}_N}{\partial\omega} + \frac{1}{2}\left(A\,\frac{\partial\mathbf{a}_N}{\partial\omega}\right)_\tau\right) \tag{6.1}$$

gives the particular solution to (3.16) shown as (3.20).

Derivation of the regularization term (3.24). Direct substitution of (3.5, 3.8, 3.14, 3.21) into the solvability condition (3.23) results in

$$-\frac{k}{2}\left(\frac{1}{\omega}\right)_\tau\left(\frac{A}{\omega}\right)_\tau - \frac{\omega}{k}(2m\partial_\zeta + m_\zeta)\left(A_\tau + \frac{\omega}{2}\left(\frac{A}{\omega}\right)_\tau\right) + \frac{\omega}{k}(\omega A)_{\zeta\zeta} + \frac{\omega^2}{k}AR = 0\ ,$$

where the $A_{\tau\tau}$ terms have identically cancelled by virtue of our choice of homogeneous contribution in $\mathbf{a}_1$. Elimination of A_τ-terms using the transport relation (3.18), yields

$$\begin{aligned} R &= \frac{3}{4k^2}\frac{1}{\omega A}(2m\partial_\zeta + m_\zeta)\left\{\omega^2(2m\partial_\zeta + m_\zeta)(\omega A)\right\} \\ &- \frac{m}{2}\left(\frac{1}{\omega}\right)_{\tau\zeta} + \frac{k^2}{4\omega^2}\left(\frac{1}{\omega}\right)_\tau\left(\frac{1}{\omega}\right)_\tau - \frac{(\omega A)_{\zeta\zeta}}{\omega A}. \end{aligned} \tag{6.2}$$

Lastly, an implicit τ-derivative of the dispersion relation (3.12) leads to the exact expression

$$\left(\frac{1}{\omega}\right)_\tau \;=\; -\frac{m\omega}{k^2}\,\omega_\zeta + \epsilon^2\frac{\omega}{2k^2}\,R_\tau \;=\; c\left(\frac{1}{\omega}\right)_\zeta + \epsilon^2\frac{\omega}{2k^2}R_\tau \tag{6.3}$$

where only the leading-order part is kept in our final equation for R (3.24).

Derivation of the frequency correction (5.8). The integrating factor step that obtains (3.19) is based upon the transport identity

$$\frac{\omega}{k}(2m\partial_\zeta + m_\zeta)\left(\frac{\omega}{k}A\right) = -\left(\frac{c}{\omega}\right)A_\zeta - \left(\frac{c}{\omega}A\right)_\zeta \tag{6.4}$$

which holds for all A. Applying this identity twice on the first term of (6.2) allows the following re-organization of terms

$$\begin{aligned}\frac{\omega^3}{k^2}\,R \;&=\; \frac{\omega}{A}\left\{\left(\frac{3c^2}{\omega^2}-\frac{\omega^2}{k^2}\right)A_\zeta\right\}_\zeta + 2\gamma \\ &\sim\; \frac{\omega}{A}\left\{\left(\frac{C'}{\Omega}\right)A_\zeta\right\}_\zeta + 2\gamma\;.\end{aligned} \tag{6.5}$$

Where the 2γ subsumes all of the A-independent terms

$$2\gamma = \frac{3}{4}\left\{\left(\frac{c}{\omega}\right)\left(\frac{c}{\omega}\right)_{\zeta\zeta} + \left(\frac{c}{\omega}\left(\frac{c}{\omega}\right)_\zeta\right)_\zeta\right\} + \frac{c}{2}\left(\frac{1}{\omega}\right)_{\tau\zeta} + \frac{\omega}{4}\left(\frac{1}{\omega}\right)_\tau\left(\frac{1}{\omega}\right)_\tau - \frac{\omega^2\omega_{\zeta\zeta}}{k^2}\;, \tag{6.6}$$

and the simplification to (6.5) occurs via a derivative of the leading-order group velocity (3.10),

$$C'(m) = \frac{dC}{dm} = \frac{3C^2}{\Omega} - \frac{\Omega^3}{k^2}\;. \tag{6.7}$$

Lastly, the (moving) complex envelope $\tilde{\Psi}$ is introduced into (6.5) by replacing the gradients of A using (5.2) and (5.6)

$$A_\zeta e^{i\Phi} \;=\; \left(\tilde{\Psi}_{\tilde{\zeta}} - i\,\frac{m-m_0}{\epsilon}\,\tilde{\Psi}\right)e^{i/\epsilon(m_0\zeta-\Omega_0\tau)} \tag{6.8}$$

which is an $O(1)$ operator local to the central characteristic (where $m - m_0 = O(\epsilon)$), and leads to the final form of the envelope equation (5.9, 5.10) shown in Section 5.

Acknowledgments. DJM thanks Nils Wedi for initiating this study of gravity wave breakdown, and the MMM Division of NCAR for their hospitality during some of the researches for this work. DJM was supported by NSERC RGPIN-238928 and NSF CMG-0327658.

REFERENCES

[1] C. M. Bender and S. A. Orszag, *Advanced Mathematical Methods for Scientists and Engineers*, McGraw-Hill, 1978.

[2] F. P. Bretherton, *Propagation in slowly varying waveguides*, Proc. Roy. Soc. A, 302, pp. 555–576 (1968).

[3] F. P. Bretherton and C. J. R. Garrett, *Wavetrains in inhomogeneous moving media*, Proc. Roy. Soc. A, 302, pp. 529–554 (1968).
[4] F. P. Bretherton, *On the mean motion induced by internal gravity waves*, J. Fluid Mech., 36, pp. 785–803 (1969).
[5] F. P. Bretherton, *The Generalised Theory of Wave Propagation*, in Mathematical Problems in the Geophysical Sciences, 1. Geophysical Fluid Dynamics, W. H. Reid ed., Lectures in Applied Mathematics, Vol. 13, American Mathematical Society, Providence, RI, 1971, pp. 61–102.
[6] P. Deift, S. Venakides and X. Zhou, *The Collisionless Shock Region for the Long Time Behavior of the Solutions of the KdV Equation*, Comm. Pure Appl. Math., 47, (1994), pp. 199-206.
[7] P. G. Drazin, *Non-linear internal gravity waves in a slightly stratified atmosphere*, J. Fluid Mech., 36, pp. 433–446 (1969).
[8] T. J. Dunkerton, *The role of gravity waves in the quasi-biennial oscillation*, J. Geophys. Res., 102, pp. 26,053-26,076 (1997).
[9] A. E. Gill, *Atmosphere-Ocean Dynamics*, Academic Press, 1982.
[10] A.V. Gurevich and L.P. Pitaevskii., *Nonstationary structure of a collisionless shock wave*, Sov. Phys. JETP, 38, pp. 2917 (1974).
[11] R. Grimshaw, *Nonlinear internal gravity waves in a slowly varying medium*, J. Fluid Mech., 54, pp. 193–207 (1972).
[12] R. Grimshaw, *Internal Gravity Waves in a Slowly Varying, Dissipative Medium*, Geophys. Fluid. Dyn., 6, pp. 131–148 (1974).
[13] R. Grimshaw, *Nonlinear Internal Gravity Waves and their Interaction with the Mean Wind*, J. Atmos. Sci., 32, pp. 1779–1793 (1975).
[14] J. Guckenheimer and P. Holmes, *Nonlinear Oscillations, Dynamical Systems, and Bifurcations of Vector Fields*, Springer-Verlag, New York, 1983.
[15] E. Hopf, *The partial differential equation* $u_t + uu_x = \mu u_{xx}$, Comm. Pure Appl. Math., 3, pp. 201–230 (1950).
[16] J. R. Holton and R. S. Lindzen, *An Updated Theory for the Quasi-Biennial Cycle of the Tropical Stratosphere* , J. Atmos. Sci., 29, pp. 1076–1080 (1972).
[17] T. Hou and P. D. Lax, *Dispersive Approximation in Fluid Dynamics*, Comm. Pure Appl. Math., 44, pp. 1–40 (1991).
[18] J. Kevorkian and J. D. Cole, *Multiple Scale and Singular Perturbation Methods*, Springer-Verlag, New York, 1996.
[19] P. D. Lax and C. D. Levermore, *The Small Dispersion Limit of the Korteweg-deVries Equation I*, Comm. Pure Appl. Math., 36, pp. 253–290 (1983).
[20] P. D. Lax and C. D. Levermore, *The Small Dispersion Limit of the Korteweg-deVries Equation II*, Comm. Pure Appl. Math., 36, pp. 571–593 (1983).
[21] M. J. Lighthill and G. B. Whitham, *On Kinematic Waves. I. Flood Movement in Long Rivers*, Proc. Roy. Soc. A, 229, pp. 281–316 (1955).
[22] J. C. Luke, *A perturbation method for nonlinear dispersive waves*, Proc. Roy. Soc. A, 292, pp. 403–412 (1966).
[23] J. C. McWilliams, *Fundamentals of Geophysical Fluid Dynamics*, Cambridge University Press, 2006.
[24] R. M. Miura and M. D. Kruskal, *Application of a Non Linear WKB Method to the Korteweg-DeVries Equation*, SIAM J. Appl. Math, 26, pp. 376–395 (1974).
[25] A. C. Newell, *Solitons in Mathematics and Physics*, SIAM, 1985.
[26] L. A. Ostrovsky and A. S. Potapov, *MODULATED WAVES: Theory and Applications*, Johns Hopkins, 1999.
[27] J. Pedlosky, *Geophysical Fluid Dynamics*, Springer-Verlag, 1987.
[28] R. A. Plumb, *The Interaction of Two Internal Wave with the Mean Flow: Implications for the Theory of the Quasi-Biennial Oscillation* , J. Atmos. Sci., 35, pp. 1847–1858 (1977).
[29] R. A. Plumb and D. McEwan, *The instability of a forced standing wave in a viscous stratified fluid: A laboratory analogue of the quasi-biennial oscillation* , J. Atmos. Sci., 35, pp. 1827–1839 (1978).
[30] C. Staquet and J. Sommeria, *INTERNAL GRAVITY WAVES: From Instabilities to Turbulence* , Ann. Rev. Fluid Mech., 34, pp. 559–593 (2002).
[31] B. R. Sutherland, *Finite-amplitude internal wavepacket dispersion and breaking*, J. Fluid Mech., 429, pp. 343–380 (2001).
[32] B. R. Sutherland, *Internal wave instability: Wave-wave versus wave-induced mean flow interactions*, Phys. Fluids, 18, 074107 (2006).
[33] B. R. Sutherland, *Weakly nonlinear internal gravity wavepackets*, J. Fluid Mech., 569,

pp. 249–258 (2006).
[34] A. Tabaei and T. R. Akylas, *Resonant long-short wave interactions in an unbounded rotating stratified fluid*, Stud. Appl. Math., 119, pp. 271–296 (2007).
[35] G. K. Vallis, *Atmospheric and Oceanic Fluid Dynamics*, Cambridge University Press, 2006.
[36] N. P. Wedi and P. K. Smolarkiewicz, *Direct Numerical Simulation of the Plumb-McEwan Laboratory Analog of the QBO*, J. Atmos. Sci., 63, pp. 3226–3252 (2006).
[37] G. B. Whitham, *A note on group velocity*, J. Fluid Mech., 9, pp. 347–352 (1960).
[38] G. B. Whitham, *Non-linear dispersive waves*, Proc. Roy. Soc. A, 292, pp. 238–261 (1965).
[39] G. B. Whitham, *A general approach to linear and non-linear dispersive waves using a Lagrangian*, J. Fluid Mech., 22, pp. 273–283 (1965).
[40] G. B. Whitham, *Two-timing, variational principles and waves*, J. Fluid Mech., 44, pp. 373–395 (1970).
[41] G. B. Whitham, *Linear and Nonlinear Waves*, Wiley, 1974.